

Searching for signatures around 1920 MeV of a N^* state of three hadron nature

A. Martínez Torres^{1*}, K. P. Khemchandani^{2†}, Ulf-G. Meißner^{3,4‡} and E. Oset^{1§}

¹*Departamento de Física Teórica and IFIC, Centro Mixto Universidad de Valencia-CSIC,
Institutos de Investigación de Paterna, Aptdo. 22085, 46071 Valencia, Spain*

²*Centro de Física Teórica, Departamento de Física,
Universidade de Coimbra, P-3004-516 Coimbra, Portugal.*

³*Helmholtz-Institut für Strahlen-und Kernphysik and Bethe Center for Theoretical Physics,
Universität Bonn, D-53115 Bonn, Germany.*

⁴*Institut für Kernphysik, Institute for Advanced Simulations and Jülich Center for Hadron Physics
Forschungszentrum Jülich, D-52425 Jülich, Germany.*

February 20, 2013

Abstract

We provide a series of arguments which support the idea that the peak seen in the $\gamma p \rightarrow K^+ \Lambda$ reaction around 1920 MeV should correspond to the recently predicted state of $J^P = 1/2^+$ as a bound state of $K\bar{K}N$ with a mixture of $a_0(980)N$ and $f_0(980)N$ components. At the same time we propose polarization experiments in that reaction as a further test of the prediction, as well as a study of the total cross section for $\gamma p \rightarrow K^+ K^- p$ at energies close to threshold and of $d\sigma/dM_{inv}$ for invariant masses close to the two kaon threshold.

*amartine@ific.uv.es

†kanchan@teor.fis.uc.pt

‡meissner@itkp.uni-bonn.de

§oset@ific.uv.es

1 Introduction

The theoretical interest in three-hadron systems other than the traditional three-nucleon states is old. In [1] there was a study of a possible system of $K\pi N$, based only on symmetries. More recently, a possible $\bar{K}NN$ bound state has been the object of intense study [2–5]. However, lately there has been a qualitative step forward in this topic, made possible by combining elements of unitarized chiral perturbation theory $U\chi PT$ [6–12] with Faddeev equations in coupled channels [13]. In [13, 14] systems of two mesons and one baryon with strangeness $S = -1$ were studied, finding resonant states which could be identified with the existing low-lying baryonic $J^P = 1/2^+$ resonances, two Λ and four Σ states. Similarly, in the case of the $S = 0$ sector the $N^*(1710)$ appears neatly as a resonance of the $\pi\pi N$ system, as well as including the channels coupled to $\pi\pi N$ within $SU(3)$ [15]. Further studies, including a realistic πN amplitude beyond the $N^*(1535)$ region to which the chiral theories are limited, give rise to other $S = 0$, $J^P = 1/2^+$ states, more precisely, the $N^*(2100)$ and the $\Delta(1910)$ [16]. Developments along the same direction produced a resonant state of $\phi K\bar{K}$ [17] which could be identified with the $X(2175)$ resonance reported by the BABAR collaboration [18, 19] and later at BES [20].

Independently, there have been similar ground-breaking studies based on variational methods [21, 22]. In particular, in Ref. [21] a bound state of $K\bar{K}N$ with $I = 1/2$, $J^P = 1/2^+$ was found around 1910 MeV in the configuration $a_0(980)N$, suggesting a bound state of the $a_0(980)$ and a nucleon. Since the $K\bar{K}$ system couples to $\pi\pi$ and $\eta\pi$ to generate the $f_0(980)$ and $a_0(980)$ resonances, a more complete coupled channels study using Faddeev equations was called for, and this was done in [16] where it was concluded that a state appears indeed around this energy, mostly made of $K\bar{K}N$ but in a mixture of $a_0(980)N$ and $f_0(980)N$.

A N^* state with these characteristics is not catalogued in the PDG [23]. However, there is a peak in the $\gamma p \rightarrow K^+\Lambda$ reaction at around 1920 MeV, clearly visible in the integrated cross section and also at all angles from forward to backward [24–26]. The $\gamma p \rightarrow K^+\Lambda$ reaction has been the object of intense theoretical study [27–31] (see [32] for a recent review). With respect to our present investigation, the possible signal for a new resonance from the peak of the cross section around 1920 MeV was already suggested in [28]. However, no spin and parity assignment were given, since there were several candidates in this region related to the missing resonances of the quark models. Other theoretical studies do not make use of this extra state, as in [29], although in this latter work only resonances with mass up to 1800 MeV were included¹. In a recent combined analysis of the $\gamma p \rightarrow K^+\Lambda$ reaction with other reactions [34], a claim for a N^* resonance around 1900 MeV was made, however, the resonance was assumed to have $J^P = 3/2^+$. Note in this respect that the PDG quotes in its latest edition that there is no evidence for this resonance in the latest analysis of the GWU group [35]. The state around this energy found in [16, 21] has instead $J^P = 1/2^+$ quantum numbers.

As one can see, the situation concerning this state and its possible nature is far from

¹Work to include more resonances in the approach of [29] is underway [33]

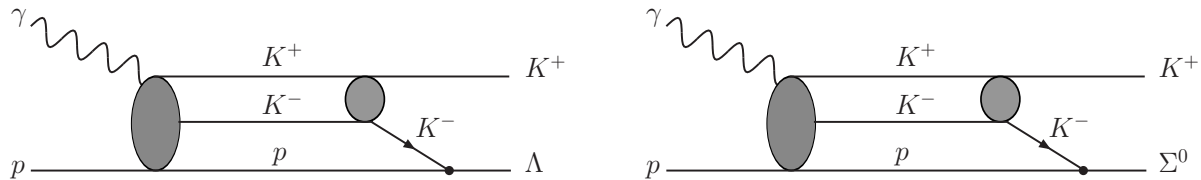


Figure 1: Diagrams depicting the $\gamma p \rightarrow K^+\Lambda$, $\gamma p \rightarrow K^+\Sigma^0$ processes through the $1/2^+$ N^* K^+K^-N resonance of [16, 21].

settled. In the present work we collect several arguments to make a case in favor of the state predicted in [16, 21] with $J^P = 1/2^+$.

2 Comparison of the $\gamma p \rightarrow K^+\Lambda$ and $\gamma p \rightarrow K^+\Sigma^0$ reactions

A peak of moderate strength on top of a large background is clearly seen for the $\gamma p \rightarrow K^+\Lambda$ reaction around 1920 MeV at all angles (see Fig. 18 of [25]). One can induce qualitatively a width for this peak of about 100 MeV or less. On the other hand, if one looks at the $\gamma p \rightarrow K^+\Sigma^0$ reaction, one finds that starting from threshold a big large and broad structure develops, also visible at all angles (see Fig. 19 of [25]). The width of this structure is about 200-300 MeV. One can argue qualitatively that the relatively narrow peak of the $\gamma p \rightarrow K^+\Lambda$ reaction around 1920 MeV on top of a large background has nothing to do with the broad structure of $\gamma p \rightarrow K^+\Sigma^0$ around 1900 MeV. A more quantitative argument can be provided by recalling that in [36] the broad structure of the $\gamma p \rightarrow K^+\Sigma^0$ is associated to two broad Δ resonances in their model, which obviously can not produce any peak in the $\gamma p \rightarrow K^+\Lambda$ reaction, which filters isospin 1/2 in the final state. Certainly, part of the structure is background, which is already obtained in chiral unitary theories at the low energies of the reaction [27].

We thus adopt the position that the peak in the $\gamma p \rightarrow K^+\Lambda$ reaction is a genuine isospin 1/2 contribution which does not show up in the $\gamma p \rightarrow K^+\Sigma^0$ reaction. This feature would find a natural interpretation in the picture of the state proposed in [16, 21]. Indeed, in those works the state at 1920 MeV is a $K\bar{K}N$ system in relative s-waves for all pairs. The $\gamma p \rightarrow K^+\Lambda$ and $\gamma p \rightarrow K^+\Sigma^0$ reactions proceeding through the excitation of this resonance are depicted in Fig. 1. The two reactions are identical in this picture, the only difference being the Yukawa coupling of the K^- to the proton to generate either a Λ or a Σ^0 .

The Yukawa couplings in SU(3) are well known and given in terms of the F and D coefficients [37], with $D + F = 1.26$ and $D - F = 0.33$ [38, 39]. The particular couplings for $K^-p \rightarrow \Lambda$ and $K^-p \rightarrow \Sigma^0$ are e.g. given in [40].

$$V_{K^-p \rightarrow \Lambda} = -\frac{2}{\sqrt{3}} \frac{D+F}{2f} + \frac{1}{\sqrt{3}} \frac{D-F}{2f}$$

(1)

$$V_{K^-p \rightarrow \Sigma^0} = \frac{D - F}{2f}$$

with f the pion decay constant. Hence, the couplings are proportional to -1.26 and 0.33 for the $K^-p \rightarrow \Lambda$ and $K^-p \rightarrow \Sigma^0$ vertices, respectively. Therefore, it is clear that in this picture the signal of the resonance in the $\gamma p \rightarrow K^+\Lambda$ reaction is far larger than in the $\gamma p \rightarrow K^+\Sigma^0$ one, by as much as an order of magnitude in the case that the resonance and background contributions sum incoherently. The $3/2^+$ resonance used in the analysis of the $\gamma p \rightarrow K^+\Lambda$ reaction in [34] is also used for the $\gamma p \rightarrow K^+\Sigma^0$ reaction in that work and also give a smaller contribution in this latter case. In the picture of [16,21] the $1/2^+$ resonance also appears in the $\gamma p \rightarrow K^+\Sigma^0$ reaction but with a smaller intensity than in the $\gamma p \rightarrow K^+\Lambda$ one, as we have mentioned.

3 Pion induced reactions

The fact that a N^* resonance around 1900 MeV is not reported in the PDG tables finds a natural interpretation in the picture of [16,21]. Indeed, since most of the information about resonances is obtained from πN reactions, it is easy to understand why this resonance did not appear in these reactions. Once again, in the picture of [16,21], the pion induced reactions going through the resonance would proceed in a direct way as shown in Fig. 2a.

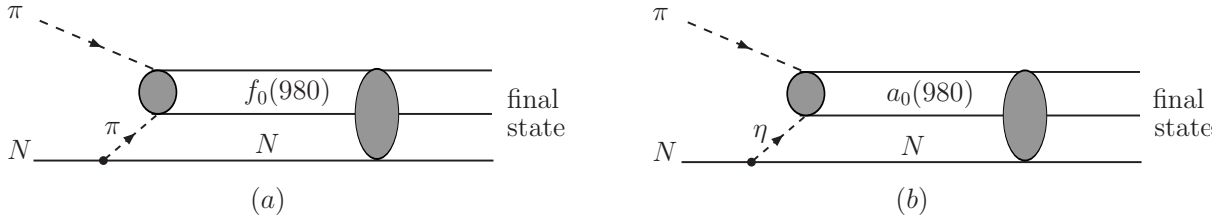


Figure 2: Diagrams for π induced reactions exciting the $1/2^+$ resonance of [16,21].

As we can see from that figure, the fact that the $f_0(980)$ has a small coupling to $\pi\pi$ [8], reflected in its small decay width, necessarily weakens the strength of the pion induced reactions producing the resonance, compared to other processes. Since the wave function of the state has also an $a_0(980)N$ component, in this case the mechanism would be the one of Fig. 2b, since the $a_0(980)N$ has also a small coupling to $\eta\pi$. Thus, the smallness of this coupling, and also the small ηNN coupling (see e.g. Ref. [41]), make again the mechanism of production very weak.

It is possible to devise some indirect method to create the $Nf_0(980)/a_0(980)$ intermediate states. One can devise the mechanisms of Fig. 3. The diagram of Fig. 3a involves the $\pi N \rightarrow K\Lambda(1405)$ transition while the one of Fig. 3b involves the $\pi N \rightarrow K\Lambda$ one. The strength of the former amplitude is much weaker than that of the second one as one can induce from experimental cross sections [42,43] and the associated amplitudes [44,45].

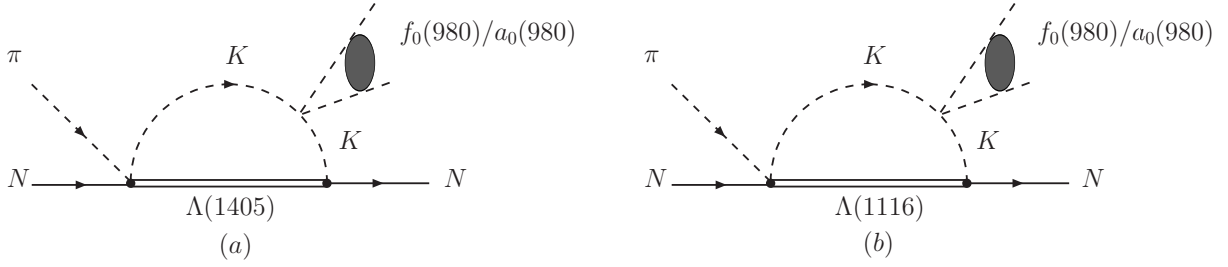


Figure 3: Possible indirect mechanism for the $\pi N \rightarrow N f_0(980)/a_0(980)$.

However, the second term is penalized by the p -wave coupling $KN\Lambda$ in the loop, where the two other vertices are in s -wave. As a general rule, loops are reduced with respect to tree level amplitudes, but in the present case the structure of these loops, with a meson-meson \rightarrow meson-meson vertex, makes the contribution very small as a direct evaluation of the diagrams shows [46].

In this respect it is also very illustrative to see that in [34] a large set of reactions was analyzed, and in Table 1 of the paper it was shown that the resonance around 1900 MeV had a weight bigger than 1 % only in the $\gamma p \rightarrow K^+\Lambda$ and $\gamma p \rightarrow K^+\Sigma^0$ reactions. This means that the weight of this resonance in the $\gamma p \rightarrow \pi N$, $\gamma p \rightarrow \eta N$, $\gamma p \rightarrow \pi\pi N$, $\gamma p \rightarrow \pi\eta N$ and $\pi N \rightarrow \pi\pi N$, analysed there, is negligible. This would again find a natural explanation along the lines discussed above if one looks at the mechanisms for these reactions depicted in Fig. 4 which are all suppressed, since they always involve the coupling of the $f_0(980)$ to $\pi\pi$ or the $a_0(980)$ to $\pi\eta$.

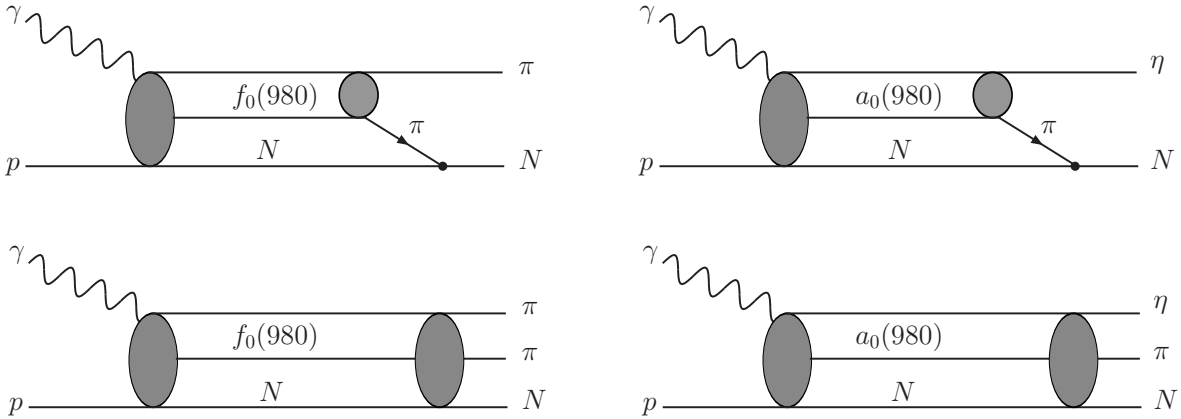


Figure 4: Diagrammatic representation of the γ induced reactions through the $1/2^+ N^*$ resonance of [16, 21] with πN , ηN , $\pi\pi N$ or $\eta\pi N$ in the final state.

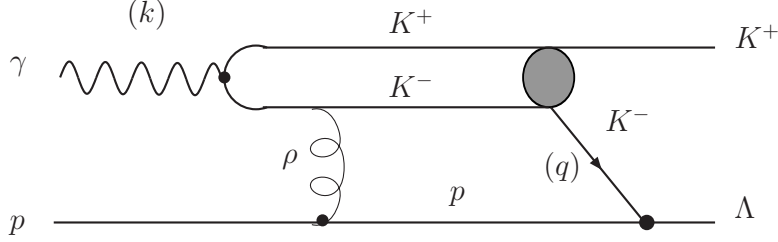


Figure 5: Schematic amplitude for $\gamma p \rightarrow K^+ \Lambda$ exciting the $1/2^+$ N^* resonance of [16, 21].

4 Angular distributions

In this section we make a different argumentation in favor of the interpretation of the state of [16, 21]. We study the angular dependence of the $\gamma p \rightarrow K^+ \Lambda$ proceeding through the resonance excitation. In order to get the basic structure of the amplitude with the quantum numbers of the resonance we take a typical mechanism compatible with the nature of the resonance as having $K\bar{K}$ in s-wave and in relative s-wave with the nucleon. This is shown in Fig. 5

The structure of the amplitude, close to $K^+ K^- p$ threshold, is given by

$$t^{(1/2)} \propto \vec{\sigma} \vec{q} \left(\frac{\vec{\sigma} \times \vec{k}}{2M_N} \right) \vec{\epsilon} \quad (2)$$

where q ($\vec{q} = -\vec{q}_{K^+}$) and k are depicted in the figure, M_N is the nucleon mass and $\vec{\epsilon}$ is the photon polarization vector. The amplitude can be rewritten as

$$t^{(1/2)} \propto \vec{\epsilon} (\vec{q} \times \vec{k}) + i \vec{\epsilon} \vec{q} \vec{\sigma} \vec{k} - i \vec{\epsilon} \vec{\sigma} \vec{k} \vec{q} \quad (3)$$

Summing the modulus squared of the amplitude over initial and final polarizations of the nucleons and the photons one obtains

$$\overline{\sum} \sum |t^{(1/2)}|^2 \propto 2 \vec{q}^2 \vec{k}^2 \quad (4)$$

and we see that there is no angular dependence.

Next we assume that we have a $J^P = 3/2^+$ state and we show in Fig. 6 the equivalent diagram to that in Fig. 5, but assuming a $J^P = 3/2^+$ baryonic intermediate state coupled to $K\bar{K}$. The amplitude has now the structure

$$t^{(3/2)} \propto \vec{S} \vec{q} \left(\frac{\vec{S}^\dagger \times \vec{k}}{2M_N} \right) \vec{\epsilon} \quad (5)$$

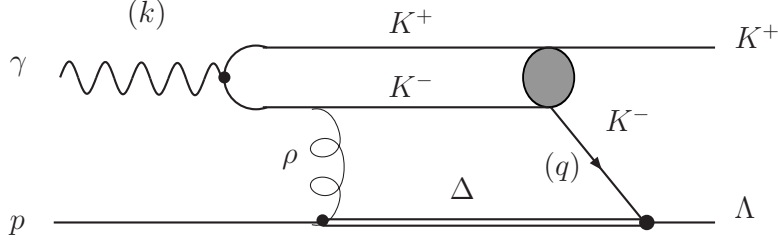


Figure 6: Schematic amplitude for $\gamma p \rightarrow K^+ \Lambda$ exciting a $3/2^+$ Δ intermediate state.

with \vec{S} the spin transition operator from spin $3/2$ to spin $1/2$. We can rewrite the amplitude taking into account the relationship

$$\sum_{M_S} S_i |M_S\rangle \langle M_S| S_j^\dagger = \frac{2}{3} \delta_{ij} - \frac{i}{3} \epsilon_{ijk} \sigma_k \quad (6)$$

and find

$$t^{(3/2)} \propto \frac{2}{3} \vec{\epsilon} (\vec{q} \times \vec{k}) - \frac{i}{3} \vec{\epsilon} \vec{q} \vec{\sigma} \vec{k} + \frac{i}{3} \vec{\epsilon} \vec{\sigma} \vec{k} \vec{q} \quad (7)$$

Upon sum of the modulus square of the amplitudes over initial and final spins we find now

$$\overline{\sum} \sum |t^{(3/2)}|^2 \propto \frac{1}{9} \vec{k}^2 \vec{q}^2 (3 \sin^2 \theta + 2) \quad (8)$$

We see that now we have a strong angular dependence and the biggest strength is expected for $\theta = 90$ degrees.

Although we have extracted the angular dependence from the particular model of Figs. 5, 6, the results are general for $\gamma N \rightarrow R \rightarrow K \Lambda$ with R a $1/2^+$ or a $3/2^+$ resonance, as one would get from the tree level amplitudes of Fig. 7 using the standard γNN , PNN , γNR , PNR vertices, with P standing for a pseudoscalar meson [47].

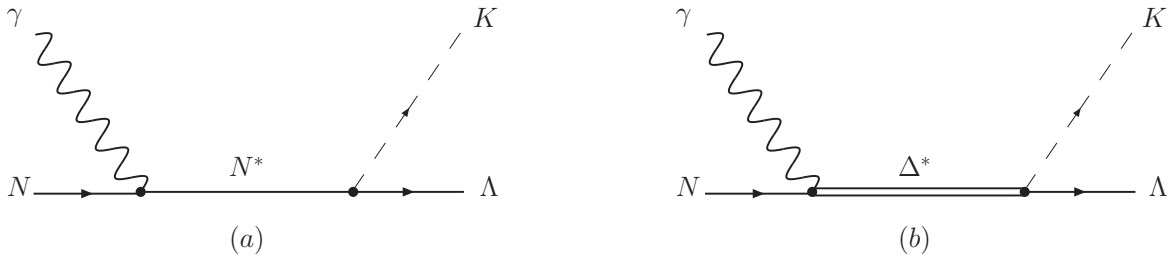


Figure 7: Diagrams for the process $\gamma N \rightarrow N^* \rightarrow K \Lambda$ (a) and $\gamma N \rightarrow \Delta^* \rightarrow K \Lambda$ (b).

Next we would like to recall what happens experimentally. As one can see in Ref. [25], the signal around 1920 MeV is present at all angles and one finds roughly a contribution of the peak around 1920 MeV over a smooth background of the order of $0.5 \mu b$ for $d\sigma/d\cos\theta$ at all angles. This would disfavor the association of the peak to a $3/2^+$ resonance, since in this case at 90 degrees one would expect the maximum signal of the resonance, with a strength about 5/2 the size of the one at forward or backward angles. The argument assumes that signal and background will sum incoherently in the reaction, which does not have to be necessarily correct, but one does not expect much coherence either in view of the many mechanisms contributing to the background in the theoretical models.

We have also given some thought to the possible use of the asymmetries already measured for this reaction [26, 48]. It is easy to see that the asymmetry, Σ , for the amplitude of our $1/2^+$ state given by Eq. (2) is $\Sigma = 0$. With this value of Σ , and assuming the contribution of the peak of the state over the background of about 20%, we find that adding the contribution of the $1/2^+$ signal Σ is reduced by about 20%. Considering that the values measured for Σ in [26, 48] have less precision than the cross sections, $\Sigma \simeq 0.25 \pm 0.15$, the changes induced in Σ by the $1/2^+$ signal are of no much help.

5 Test with polarization experiments

In case the $J^P = 1/2^+$ assignment was correct, an easy test can be carried out to rule out the $3/2^+$ state. The experiment consists in performing the $\gamma p \rightarrow K^+ \Lambda$ reaction with a circularly polarized photon with helicity 1, thus $S_z = 1$ with the z -axis defined along the photon direction, together with a polarized proton of the target with $S_z = 1/2$ along the same direction. With this set up, the total spin has $S_z^{tot} = 3/2$. Since L_z is zero with that choice of the z direction, then $J_z^{tot} = 3/2$ and J must be equal or bigger than $3/2$. Should the resonant state be $J^P = 1/2^+$, the peak signal would disappear for this polarization selection, while it would remain if the resonance was a $J^P = 3/2^+$ state. Thus, the disappearance of the signal with this polarization set up would rule out the $J^P = 3/2^+$ assignment.

Such type of polarization set ups have been done and are common in facilities like ELSA at Bonn, MAMI B at Mainz or CEBAF at Jefferson Lab, where spin-3/2 and 1/2 cross sections, which play a crucial role in the GDH sum rule, see e.g. Ref. [49], were measured in the two-pion photoproduction [50, 51] reaction. The theoretical analysis of [52] shows indeed that the separation of the amplitudes in the spin channels provides information on the resonances excited in the reaction.

6 Analysis of the reaction $\gamma p \rightarrow K^+ K^- p$ close to threshold

An ideal test of the nature of the resonance predicted around 1920 MeV is the study of the process $\gamma p \rightarrow K^+ K^- p$ close to threshold. This reaction has received relatively good

experimental attention [53–56], stimulated recently by the search of a possible pentaquark state of strangeness $S=1$. Theoretically it has also been studied in [57–61], also motivated by the search of the pentaquark of strangeness $S = 1$, or the nature of the $\Lambda(1520)$ and other resonances. Yet, the emphasis here is different and the measurements required are very close to threshold, in the region below the ϕ production to avoid unnecessary complications in the analysis. Indeed, as we mentioned, the resonance has all the K^+K^-p components in s-wave and the energy is just a bit below the threshold of the reaction. The effect of this resonance should be seen as an accumulation of strength in the cross section close to threshold compared with phase space. Such effects are common in many reactions [62–64]. In order to see the effects expected for this case we again draw in Fig. 8 a typical diagram which would contribute to the $\gamma p \rightarrow K^+K^-p$ close to threshold through the intermediate resonance excitation.

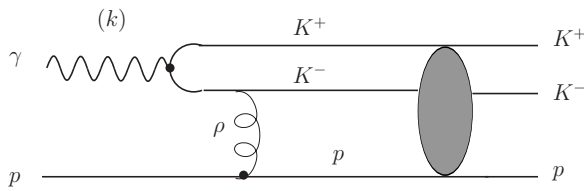


Figure 8: Schematic amplitude for $\gamma p \rightarrow K^+K^-p$ exciting the $1/2^+ N^*$ resonance of [16,21].

By looking at Fig. 8, in the shaded blob of the figure one is assuming all interactions of $K^+K^-p \rightarrow K^+K^-p$, which one encounters in a full Faddeev calculation. Hence, the amplitude for $\gamma p \rightarrow K^+K^-p$ can be written as

$$t_{prod} \propto T_{K^+K^-p \rightarrow K^+K^-p} \quad (9)$$

The $T_{K^+K^-p \rightarrow K^+K^-p}$ amplitude was evaluated using Faddeev equations in coupled channels [16]. We are assuming that this term, which exhibits the peak due to the $1/2^+ N^*$ resonance, dominates over a possible background term close to threshold (for instance, a tree level diagram like the one of Fig. 8 omitting the interaction of the particles symbolized by the shaded blob or diagrams with two-particle final-state interactions). The scheme of the latter work is very rewarding for experimental tests. Indeed, what one evaluates there is the T -matrix as a function of two variables. These are \sqrt{s} , the total energy, and $\sqrt{s_{23}}$, the invariant mass of the subsystem of two particles that one expects to be highly correlated. This is the case here, where the K^+K^- is correlated to the $a_0(980)$ and $f_0(980)$ resonances below the K^+K^- threshold, hence $\sqrt{s_{23}}$ is taken for the K^+K^- pair. Since the T amplitude of [16] does not have any angular dependence, and for a fixed total energy only depends on $\sqrt{s_{23}}$, the differential cross section for the $\gamma p \rightarrow K^+K^-p$ reaction is readily found and we have

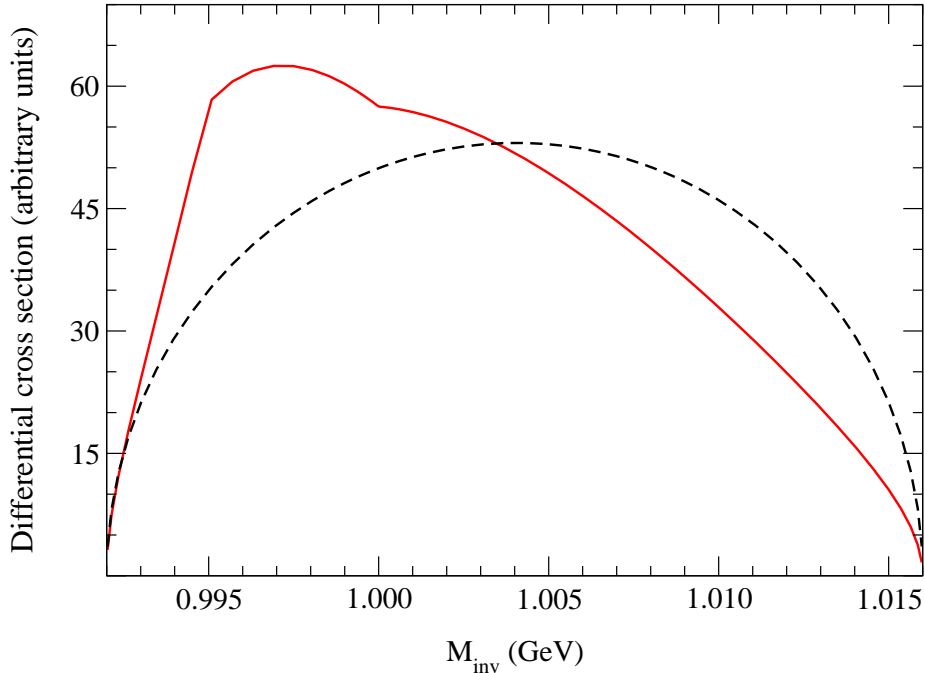


Figure 9: $d\sigma/dM_{inv}$ with phase space (dashed line) and using the $K^+K^-p \rightarrow K^+K^-p$ amplitude of [16] (solid line), with M_{inv} the invariant mass for the K^+K^- system. The curves have been normalized to have the same integrated cross section.

$$\frac{d\sigma}{dM_{inv}} = C \frac{1}{s - M_N^2} \frac{1}{\sqrt{s}} p \tilde{q} |T_{K^+K^-p \rightarrow K^+K^-p}|^2 \quad (10)$$

$$p = \frac{\lambda^{1/2}(s, M_{inv}^2, M_N^2)}{2\sqrt{s}}, \quad \tilde{q} = \frac{\lambda^{1/2}(M_{inv}^2, m_K^2, m_K^2)}{2M_{inv}} \quad (11)$$

where C is a constant and we have written M_{inv} for the invariant mass of the two-kaon system, the $\sqrt{s_{23}}$ variable in Ref. [16].

In order to show the effects of the resonance below threshold and the correlations of M_{inv} we show two plots in Figs. 9 and 10.

In Fig. 9 we take a fixed energy, just below ϕN production with $\sqrt{s} = 1955$ MeV and plot $d\sigma/dM_{inv}$ as a function of M_{inv} for phase space (dashed line) and for Eq. (10) (solid line). As we can see, there is a big asymmetry of the mass distribution with respect to phase space, with a clear accumulation of strength close to $M_{inv} = 2m_K$ as a consequence of the presence of the $f_0(980)$ or $a_0(980)$ below threshold. The results have been normalized to the same integrated cross section.

In Fig. 10, we have instead represented the integrated cross section of $\gamma p \rightarrow K^+K^-p$ as a function of the energy from threshold up to $\sqrt{s} = 1955$ MeV evaluated with Eq. (10) (solid line) and we compare the results with phase space (dashed line). The cross section have been normalized to one at $\sqrt{s} = 1955$ MeV for comparison. What we observe here

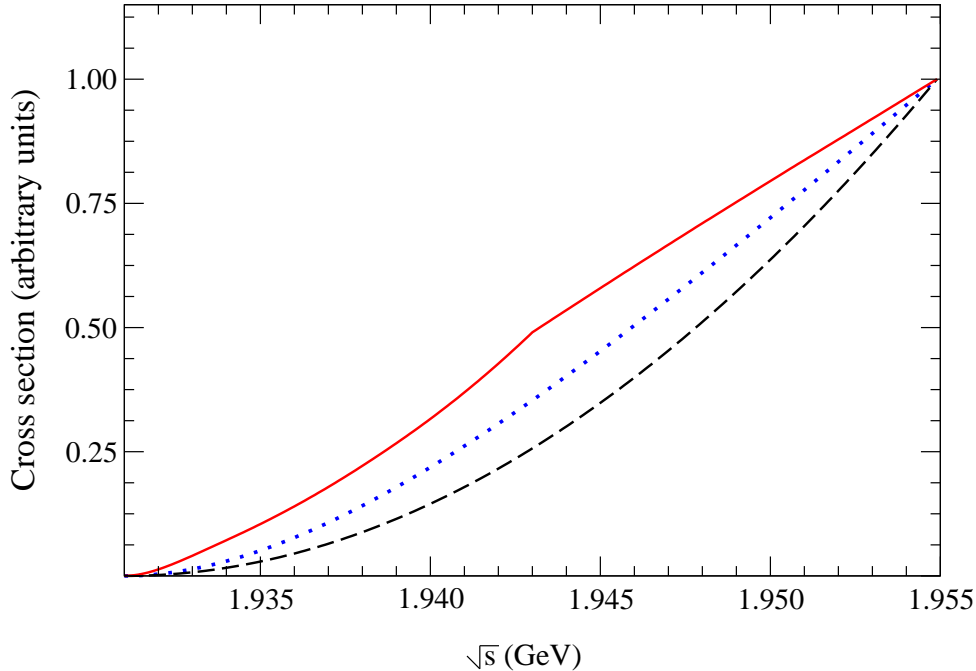


Figure 10: Integrated cross sections. Dashed line: phase space. Dotted line: using the amplitude of Eq. (12) accounting for K^+K^- final-state interaction. Solid line: results obtained using the $K^+K^-p \rightarrow K^+K^-p$ amplitude of [16]. The curves have been normalized to unity at 1955 MeV.

is that the cross section is also more pronounced at lower energies as a consequence of the presence of the three particle resonance below threshold.

We should also take into account that the shape of $d\sigma/dM_{inv}$ in Fig. 9 should be expected from final-state interactions of the K^+K^- pair close to threshold, even if the $N^*(1920)$ resonance were not present [62–64]. This means that instead of phase space we should already consider a T matrix element accounting for the K^+K^- final-state interaction incorporating the pole of the $f_0(980)$ or $a_0(980)$. Thus we perform the evaluation of the cross section with an empirical amplitude

$$t_{prod} \propto \frac{1}{M_{inv}^2 - M_{f_0}^2 + i\Gamma_{f_0} M_{f_0}} \quad (12)$$

with $M_{f_0} = 980$ MeV and $\Gamma_{f_0} = 30$ MeV. We note that using this amplitude we obtain a distribution $d\sigma/dM_{inv}$ very similar to the one obtained in Fig. 9 using the amplitude of [16]. The results for the integrated cross section with the amplitude of Eq. (12) can be seen in the dotted line in Fig. 10. We can still see deviations from the new curve incorporating the K^+K^- final-state interaction with respect to the curve accounting for the $N^*(1920)$ resonance in addition (solid curve in Fig. 10).

In the calculations of Ref. [16] the width obtained, of around 20 MeV, should be smaller than the one of the real state because one only has three-body states and the decay into

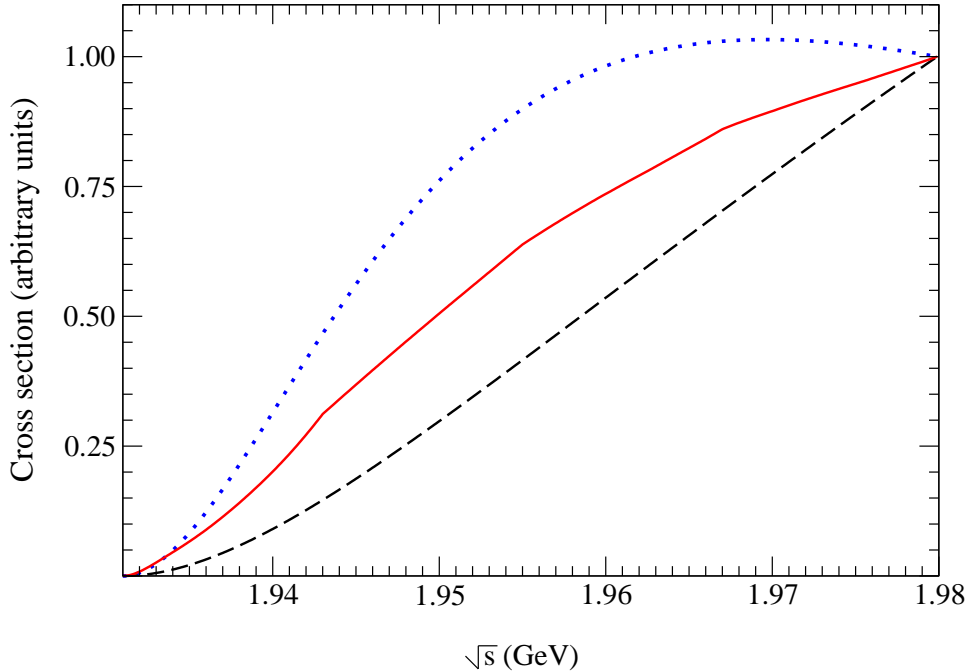


Figure 11: Integrated cross sections. Dashed line: using the amplitude of Eq. (12) which accounts for the K^+K^- final-state interaction. Solid line: results using the K^+K^-p amplitude of [16]. Dotted line: results using the empirical amplitude of Eq. (13) accounting for the K^+K^- final-state interaction plus a resonant pole at 1924 MeV with a width of 60 MeV.

two particles is not included. As discussed in [16], even if the building blocks are three particles, one can obtain a larger width for the decay into two-body systems because there is more phase space for it. Because of that, in order to estimate possible uncertainties from this deficiency, we show what we would observe if we just had a resonance below threshold with a typical Breit-Wigner amplitude with mass $M_R = 1924$ MeV and width of about 60 MeV,

$$t_{prod} \propto \frac{1}{\sqrt{s} - M_R + i\frac{\Gamma}{2}} \frac{1}{M_{inv}^2 - M_{f_0}^2 + i\Gamma_{f_0} M_{f_0}} \quad (13)$$

The problem in this case is that the span of energies chosen in Fig. 10 from threshold to 1955 MeV is only of about 25 MeV, smaller than the width, such that one can not see the resonance structure in such a narrow range any more. Going to higher energies has the problem that we should face the ϕ production which has a large cross section. A way out of this problem could be found by eliminating from the experimental cross section the very narrow peak for the ϕ production. Assuming then that there is no contribution from ϕ production we compare the result obtained with the amplitude of Eq. (12) and the one with Eq. (13) which accounts also for the $N^*(1920)$ resonant pole. We show the results in Fig. 11, where the cross sections have been normalized to one at $\sqrt{s} = 1980$ MeV.

We observe that the effect of the $N^*(1920)$ resonance is clearly visible, with an enhanced

cross section at lower energies compared with the curve that has only the K^+K^- final state. We also include in the figure the results obtained using the amplitude of Eq. (9) (solid line). The region between the two upper curves can indicate the theoretical uncertainties but we can see that, in any case, a clear enhancement due to the N^* resonance is seen.

The effects observed in this calculation call for an experimental test which could verify, or eventually refute the findings obtained above based on the nature of the predicted $1/2^+$ state around 1920 MeV. This analysis is underway at Spring8/Osaka [65].

7 Conclusions

The independent prediction, also using different methods, of a $1/2^+$ state around 1920 MeV as a bound state of $K\bar{K}N$, which appears in the $a_0(980)N$ and $f_0(980)N$ configurations, stimulated us to suggest that this state may have already been seen in the peak observed in the $\gamma p \rightarrow K^+\Lambda$ reaction around this energy. Based on the structure found in [16,21] we could explain why a relatively narrow peak appears in the $\gamma p \rightarrow K^+\Lambda$ reaction on top of a large background and it does not show up on top of the broader structure around these energies in the $\gamma p \rightarrow K^+\Sigma^0$ reaction. We could also find an easy interpretation on why the state does not show up in pion induced reactions, or in reactions with πN or ηN in the final states, because of the small coupling of the $f_0(980)N$ to $\pi\pi$ or of the $a_0(980)N$ to $\eta\pi$. In order to find extra support for the idea we suggested two experiments. One of them is the separation of the $S_z = 3/2$ and $S_z = 1/2$ parts of the $\gamma p \rightarrow K^+\Lambda$ cross section, which would rule out the $3/2^+$ assignment if there is no cross section in the $S_z = 3/2$ channel. The other one is the investigation of the cross section close to threshold and the invariant mass distributions close to the two kaon mass, which should show enhancements close to both thresholds, indicating a bound state below the $K\bar{K}N$ mass with the two kaons strongly correlated to form the $a_0(980)N$ and $f_0(980)N$ states. Both experiments are feasible in existing laboratories and we hope that the present work encourages their implementation.

Acknowledgments

We would like to thank Juan Nieves and T. Nakano for useful discussions. This work is partly supported by DGICYT contract number FIS2006-03438. We acknowledge the support of the European Community-Research Infrastructure Integrating Activity ‘‘Study of Strongly Interacting Matter’’ (acronym HadronPhysics2, Grant Agreement n. 227431) under the Seventh Framework Programme of EU. Work supported in part by DFG (SFB/TR 16, ‘‘Subnuclear Structure of Matter’’), and by the Helmholtz Association through funds provided to the virtual institute ‘‘Spin and strong QCD’’ (VH-VI-231). One of the authors (A. M. T.) is supported by a FPU grant of the Ministerio de Ciencia y Tecnología. K. P. Khemchandani thanks the support by the Fundação para a Ciência e a Tecnologia of the Ministério da Ciência, Tecnologia e Ensino Superior of Portugal (SFRH/BPD/40309/2007).

References

- [1] H. Harari and H. J. Lipkin, Phys. Rev. Lett. **13**, 345 (1964).
- [2] N. V. Shevchenko, A. Gal, J. Mares and J. Revai, Phys. Rev. C **76**, 044004 (2007) [arXiv:0706.4393 [nucl-th]].
- [3] A. Dote, T. Hyodo and W. Weise, Nucl. Phys. A **804**, 197 (2008) [arXiv:0802.0238 [nucl-th]].
- [4] Y. Ikeda and T. Sato, Phys. Rev. C **76**, 035203 (2007) [arXiv:0704.1978 [nucl-th]].
- [5] T. Yamazaki and Y. Akaishi, Phys. Rev. C **76**, 045201 (2007) [arXiv:0709.0630 [nucl-th]].
- [6] N. Kaiser, P. B. Siegel and W. Weise, Nucl. Phys. A **594**, 325 (1995) [arXiv:nucl-th/9505043].
- [7] A. Dobado and J. R. Pelaez, Phys. Rev. D **56**, 3057 (1997) [arXiv:hep-ph/9604416].
- [8] J. A. Oller and E. Oset, Nucl. Phys. A **620**, 438 (1997) [Erratum-ibid. A **652**, 407 (1999)] [arXiv:hep-ph/9702314].
- [9] J. A. Oller, E. Oset and J. R. Pelaez, Phys. Rev. D **59**, 074001 (1999) [Erratum-ibid. D **60**, 099906 (1999 ERRAT,D75,099903.2007)] [arXiv:hep-ph/9804209].
- [10] J. A. Oller and U.-G. Meißner, Phys. Lett. B **500**, 263 (2001) [arXiv:hep-ph/0011146].
- [11] C. Garcia-Recio, J. Nieves, E. Ruiz Arriola and M. J. Vicente Vacas, Phys. Rev. D **67**, 076009 (2003) [arXiv:hep-ph/0210311].
- [12] T. Hyodo, S. I. Nam, D. Jido and A. Hosaka, Phys. Rev. C **68**, 018201 (2003) [arXiv:nucl-th/0212026].
- [13] A. Martinez Torres, K. P. Khemchandani and E. Oset, Phys. Rev. C **77**, 042203 (2008) [arXiv:0706.2330 [nucl-th]].
- [14] A. Martinez Torres, K. P. Khemchandani and E. Oset, Eur. Phys. J. A **35**, 295 (2008) [arXiv:0805.3641 [nucl-th]].
- [15] K. P. Khemchandani, A. Martinez Torres and E. Oset, Eur. Phys. J. A **37**, 233 (2008) [arXiv:0804.4670 [nucl-th]].
- [16] A. Martinez Torres, K. P. Khemchandani and E. Oset, arXiv:0812.2235 [nucl-th].
- [17] A. Martinez Torres, K. P. Khemchandani, L. S. Geng, M. Napsuciale and E. Oset, Phys. Rev. D **78**, 074031 (2008) [arXiv:0801.3635 [nucl-th]].

- [18] B. Aubert *et al.* [BABAR Collaboration], Phys. Rev. D **74**, 091103 (2006) [arXiv:hep-ex/0610018].
- [19] B. Aubert *et al.* [BABAR Collaboration], Phys. Rev. D **76**, 012008 (2007) [arXiv:0704.0630 [hep-ex]].
- [20] M. Ablikim *et al.* [BES Collaboration], Phys. Rev. Lett. **100**, 102003 (2008) [arXiv:0712.1143 [hep-ex]].
- [21] D. Jido and Y. Kanada-En'yo, Phys. Rev. C **78**, 035203 (2008) [arXiv:0806.3601 [nucl-th]].
- [22] Y. Kanada-En'yo and D. Jido, Phys. Rev. C **78**, 025212 (2008) [arXiv:0804.3124 [nucl-th]].
- [23] C. Amsler *et al.* [Particle Data Group], Phys. Lett. B **667**, 1 (2008).
- [24] K. H. Glander *et al.*, Eur. Phys. J. A **19**, 251 (2004) [arXiv:nucl-ex/0308025].
- [25] R. Bradford *et al.* [CLAS Collaboration], Phys. Rev. C **73**, 035202 (2006) [arXiv:nucl-ex/0509033].
- [26] M. Sumihama *et al.* [LEPS Collaboration], Phys. Rev. C **73**, 035214 (2006) [arXiv:hep-ex/0512053].
- [27] B. Borasoy, P. C. Bruns, U. G. Meissner and R. Nissler, Eur. Phys. J. A **34**, 161 (2007) [arXiv:0709.3181 [nucl-th]].
- [28] T. Mart and C. Bennhold, Phys. Rev. C **61**, 012201 (2000) [arXiv:nucl-th/9906096].
- [29] A. Usov and O. Scholten, Phys. Rev. C **72**, 025205 (2005) [arXiv:nucl-th/0503013].
- [30] V. Shklyar, H. Lenske and U. Mosel, Phys. Rev. C **72**, 015210 (2005) [arXiv:nucl-th/0505010].
- [31] B. Julia-Diaz, B. Saghai, T. S. Lee and F. Tabakin, Phys. Rev. C **73**, 055204 (2006) [arXiv:nucl-th/0601053].
- [32] T. Mart, AIP Conf. Proc. **1056**, 31 (2008) [arXiv:0808.0771 [nucl-th]].
- [33] O. Scholten, private communication.
- [34] V. A. Nikonov, A. V. Anisovich, E. Klempt, A. V. Sarantsev and U. Thoma, Phys. Lett. B **662**, 245 (2008) [arXiv:0707.3600 [hep-ph]].
- [35] R. A. Arndt, W. J. Briscoe, I. I. Strakovsky and R. L. Workman, Phys. Rev. C **74**, 045205 (2006) [arXiv:nucl-th/0605082].

- [36] F. X. Lee, T. Mart, C. Bennhold and L. E. Wright, Nucl. Phys. A **695**, 237 (2001) [arXiv:nucl-th/9907119].
- [37] V. Bernard, N. Kaiser and U.-G. Meißner, Int. J. Mod. Phys. E **4**, 193 (1995) [arXiv:hep-ph/9501384].
- [38] F. E. Close and R. G. Roberts, Phys. Lett. B **316**, 165 (1993) [arXiv:hep-ph/9306289].
- [39] B. Borasoy, P. C. Bruns, U.-G. Meißner and R. Nissler, Eur. Phys. J. A **34**, 161 (2007) [arXiv:0709.3181 [nucl-th]].
- [40] E. Oset and A. Ramos, Nucl. Phys. A **679**, 616 (2001) [arXiv:nucl-th/0005046].
- [41] U. G. Meissner, N. Kaiser, H. Weigel and J. Schechter, Phys. Rev. D **39**, 1956 (1989) [Erratum-ibid. D **40**, 262 (1989)].
- [42] D. W. Thomas, A. Engler, H. E. Fisk and R. W. Kraemer, Nucl. Phys. B **56**, 15 (1973).
- [43] J. J. Jones *et al.*, Phys. Rev. Lett. **26**, 860 (1971).
- [44] T. Hyodo, A. Hosaka, E. Oset, A. Ramos and M. J. Vicente Vacas, Phys. Rev. C **68**, 065203 (2003) [arXiv:nucl-th/0307005].
- [45] T. Inoue, E. Oset and M. J. Vicente Vacas, Phys. Rev. C **65**, 035204 (2002) [arXiv:hep-ph/0110333].
- [46] V. K. Magas, E. Oset and A. Ramos, Phys. Rev. Lett. **95**, 052301 (2005) [arXiv:hep-ph/0503043].
- [47] R. C. Carrasco, E. Oset and L. L. Salcedo, Nucl. Phys. A **541**, 585 (1992).
- [48] R. G. T. Zegers *et al.* [LEPS Collaboration], Phys. Rev. Lett. **91**, 092001 (2003) [arXiv:nucl-ex/0302005].
- [49] D. Drechsel, Prog. Part. Nucl. Phys. **34**, 181 (1995) [arXiv:nucl-th/9411034].
- [50] J. Ahrens *et al.* [GDH Collaboration and A2 Collaboration], Phys. Rev. Lett. **87**, 022003 (2001) [arXiv:hep-ex/0105089].
- [51] J. Ahrens *et al.* [GDH and A2 Collaborations], Eur. Phys. J. A **34**, 11 (2007).
- [52] J. C. Nacher and E. Oset, Nucl. Phys. A **697**, 372 (2002) [arXiv:nucl-th/0106005].
- [53] D. P. Barber *et al.*, Z. Phys. C **7**, 17 (1980).
- [54] J. Barth *et al.*, Eur. Phys. J. A **17** (2003) 269.

- [55] V. Kubarovsky *et al.* [CLAS Collaboration], Phys. Rev. Lett. **97**, 102001 (2006) [arXiv:hep-ex/0605001].
- [56] T. Nakano [LEPS Collaboration], AIP Conf. Proc. **915** (2007) 162.
- [57] W. Roberts, Phys. Rev. C **70**, 065201 (2004) [arXiv:nucl-th/0408034].
- [58] Y. Oh, K. Nakayama and T. S. Lee, Phys. Rept. **423**, 49 (2006) [arXiv:hep-ph/0412363].
- [59] L. Roca, E. Oset and H. Toki, arXiv:hep-ph/0411155.
- [60] L. Roca, S. Sarkar, V. K. Magas and E. Oset, Phys. Rev. C **73**, 045208 (2006) [arXiv:hep-ph/0603222].
- [61] A. Sibirtsev, J. Haidenbauer, S. Krewald, U.-G. Meißner and A. W. Thomas, Eur. Phys. J. A **31**, 221 (2007) [arXiv:hep-ph/0509145].
- [62] E. Oset, J. A. Oller and U.-G. Meißner, Eur. Phys. J. A **12**, 435 (2001) [arXiv:nucl-th/0109050].
- [63] C. Hanhart, Yu. S. Kalashnikova, A. E. Kudryavtsev and A. V. Nefediev, Phys. Rev. D **76**, 034007 (2007) [arXiv:0704.0605 [hep-ph]].
- [64] A. Dzyuba, M. Buscher, C. Hanhart, V. Kleber, V. Koptev, H. Stroher and C. Wilkin, Eur. Phys. J. A **38**, 1 (2008) [arXiv:0804.3695 [nucl-ex]].
- [65] T. Nakano, private communication.